

lncRNA LUCAT1 acts as a potential biomarker and demonstrates malignant biological behaviors in gastric cancer

YangYang Teng

The Second Affiliated Hospital and Yuying Children's Hospital of Wenzhou Medical University
<https://orcid.org/0000-0002-3775-328X>

HeJie Yu

The Second Affiliated Hospital and Yuying Children's Hospital of Wenzhou Medical University

LeYi Ni

The Second Affiliated Hospital and Yuying Children's Hospital of Wenzhou Medical University

GuangRong Lu

The Second Affiliated Hospital and Yuying Children's Hospital of Wenzhou Medical University

YueSheng Zhu

The Second Affiliated Hospital and Yuying Children's Hospital of Wenzhou Medical University

LingLing Zhou

The Second Affiliated Hospital and Yuying Children's Hospital of Wenzhou Medical University

Jing Zhang

The Second Affiliated Hospital and Yuying Children's Hospital of Wenzhou Medical University

ZhanXiong Xue

The Second Affiliated Hospital and Yuying Children's Hospital of Wenzhou Medical University

ZhenZhai Cai

The Second Affiliated Hospital and Yuying Children's Hospital of Wenzhou Medical University

Chao Xing (✉ doctor_xc@163.com)

<https://orcid.org/0000-0002-8269-7141>

Research article

Keywords: gastric cancer;lncRNA;LUCAT1;biomarker;metastasis

Posted Date: May 29th, 2020

DOI: <https://doi.org/10.21203/rs.3.rs-31580/v1>

License: © ⓘ This work is licensed under a Creative Commons Attribution 4.0 International License.

[Read Full License](#)

Abstract

Gastric cancer(GC) remains the fourth-leading malignancy worldwide and has a high mortality rate. Accumulating evidence reveals that long noncoding RNAs (lncRNAs) play essential roles in tumorigenesis and metastasis and can be used as potential biomarkers for diagnosis and prognosis. The current study sought to define the lncRNA LUCAT1 and verify its malignant biological behaviors in GC. We conducted bioinformatic analysis to screen differentially expressed lncRNAs between GC tissue and paracancerous tissue. Gene expression profiles were downloaded from the National Center of Biotechnology Information Gene Expression Omnibus(GEO). Real-time quantitative polymerase chain reaction (RT-qPCR) was carried out to verify LUCAT1 expression in both GC tissue and paracancerous tissue. Furthermore, the associations between LUCAT1 and clinical features were analyzed. In addition, the malignant behaviors of LUCAT1 in GC were investigated by knocking down LUCAT1 expression in the SGC7901 and AGS cell lines. The results indicated that LUCAT1 expression was obviously upregulated in GC samples compared with paracancerous tissue samples. Moreover, the expression pattern of LUCAT1 showed close correlations with tumor diameter ($P < 0.001$), differentiation grade ($P = 0.026$), and lymphnode metastasis(LNM) status ($P = 0.020$). In vitro, shRNA-mediated knockdown of LUCAT1 expression inhibited proliferation, migration, and invasion and led to S-phase cell cycle arrest and apoptosis in GC cells. Thus, the lncRNA LUCAT1 may be used as a potential biomarker for early signs of LNM in GC and may play a crucial role in the development of GC.

Introduction

Gastric cancer (GC) is still the 4th most common malignancy and the 3rd leading cause of cancer-related death, following lung cancer and hepatic cancer[1]. Due to the development of early detection techniques and improvements in surgical treatment, the overall survival of patients with GC has gradually improved[2-4]. However, many patients are diagnosed with GC in the late stage of obvious metastasis, at which point they are no longer eligible for curative surgery. One important reason is the lack of specificity of the early clinical symptoms of GC. Thus, the search for new effective biomarkers is still essential for the early diagnosis of GC.

lncRNAs have been thought to be lacking in cellular biology because of their extremely limited protein-coding ability. In recent years, as people have focused their attention on lncRNAs, an increasing number of studies have shown that lncRNAs have close relationships with lung cancer, colorectal cancer and other malignant tumors[5, 6]. The differential expression of lncRNAs may be a new regulatory factor in cell proliferation, metastasis, apoptosis and tumor development. Competing endogenous RNA (ceRNA) networks are large-scale regulatory networks across the transcriptome that can reveal the molecular mechanisms underlying pathological conditions, such as cancer[7, 8]. Accumulating evidence indicates that lncRNAs harbor miRNA response elements (MREs) and play important roles in oncogenesis through interactions with DNA, RNA and proteins[9, 10]. However, few lncRNAs have been well characterized to date, and the biological function and clinical significance of most lncRNAs in GC remain unknown.

In this study, we identified lncRNAs, miRNAs and mRNAs related to GC through the construction of a ceRNA network and found that the expression of LUCAT1 in GC tissue was significantly higher than that in paracancerous tissue, suggesting that LUCAT1 may be an oncogene in GC. The associations between LUCAT1 and clinical features were analyzed. Furthermore, targeted depletion of LUCAT1 in AGS and SGC-7901 cells was carried out by lentivirus-mediated RNA interference, which was used to silence genes at the posttranscriptional level. The effects of LUCAT1 gene knockout on cell proliferation and clone formation were studied. In addition, the effects of LUCAT1 gene knockout on cell cycle regulation, invasion and migration were also evaluated to reveal the potential relationship between LUCAT1 and GC.

Materials And Methods

1. Differential gene expression in GC

All of the microarray datasets in the National Center of Biotechnology Information Gene Expression Omnibus (<http://www.ncbi.nlm.nih.gov/geo/>) were searched to identify differentially expressed genes. The original lncRNA, mRNA and miRNA expression profiles of the GSE84787, GSE79973 and GSE93415 datasets, respectively, were obtained. The GSE84787 and GSE79973 datasets had 10 pairs of GC tissue and paracancerous mucosal tissue samples and GSE93415, which included 20 pairs of GC tissue and matched paraneoplastic samples. The robust multi-array average algorithm was used to perform background correction and quartile data normalization of these data [11]. Only the average values of gene symbols with multiple probes were calculated, the others without corresponding symbols were filtered. Student's t-test and fold change (FC) filtering were conducted to screen differentially expressed genes (DEGs) between two groups with the R software limma package [12]. With the threshold of a P-value < 0.05 and an absolute FC value > 2, volcano plot filtering was performed using the R software ggplot2 package to identify significant DEGs between two groups.

2. Construction of an lncRNA-miRNA-mRNA network

lncRNA gene annotation was performed according to the LNCipedia database [13]. DIANA-LncBase v.2 [14] was used to predict the interactions between miRNAs and lncRNAs with a threshold prediction score > 0.8. Differentially expressed lncRNAs and predicted target lncRNAs were intersected to select differentially expressed miRNA-targeted lncRNAs. Then, the interactions between miRNAs and mRNAs were predicted by using miRtarbase [15]. Differentially expressed mRNAs and predicted target mRNAs were intersected to select differentially expressed miRNA-targeted mRNAs. Significantly expressed miRNAs and their significantly expressed targets (mRNAs and lncRNAs) were superimposed onto an lncRNA-miRNA-mRNA network. The network was constructed by Cytoscape (version 3.4.0), and its topology was analyzed with CentiScaPe app [16]. A flowchart detailing the construction of the lncRNA-miRNA-mRNA network is shown in Figure. S1.

3. Study population and specimens

This study consisted of 70 GC fresh-frozen tissue specimens and paired adjacent normal tissue specimens (at least 5 cm from the negative resection margin) obtained during surgical resections performed at the Second Affiliated Hospital of Wenzhou Medical University (Wenzhou, China) between February 2017 and February 2018. All participants were self-reported Han Chinese. Both the GC and paracancerous specimens were confirmed by histopathological diagnosis. The tumor clinicopathological data are summarized in accordance with the TNM staging system of the American Joint Committee on Cancer staging manual (8th edition). Histological grades were assessed following the National Comprehensive Cancer Network (NCCN) clinical practice guideline of oncology (V.1.2011). Patients did not receive radiotherapy, chemotherapy or targeted therapy prior to undergoing surgery. The study was authorized by the institutional review boards of the Second Affiliated Hospital of Wenzhou Medical University. Each patient provided written informed consent.

4. Cell culture

Two GC cell lines (AGS and SGC-7901) and the normal gastric mucosal cell line GES1 were purchased from the Shanghai Genechem Co., Ltd (Shanghai, China). AGS and SGC-7901 cells were cultured in DMEM containing 10% FBS in a constant-temperature humidified incubator. Generally, the medium was replaced every 2 days, and the number of cells in the medium became saturated within approximately 5 days; at this time, the cells were subcultured.

5. Total RNA extraction and reverse transcription

All fresh tissue samples were stored in a freezer at -80°C from the time they were collected to the time of use and fixed with RNA fixing reagent (Baiteke, Beijing, China). TRIzol reagent (Invitrogen, Karlsruhe, Germany) was used to quickly extract total tissue RNA from the GC tissue and adjacent nontumor tissue samples; however, as this reagent is harmful to the human body, disposable gloves were worn for protection against any spillage. The whole process was performed strictly in accordance with the manufacturer's instructions. Then, total RNA was quantified using a Scandrop100 (Analytikjena, Germany). The A260/A280 ratio was used to indicate the purity of the isolated total RNA. Most of the sample values were between 1.8 and 2.0. Then, cDNA was synthesized by reverse transcription (RT) using random primers and the TURScript 1st Stand cDNA SYNTHESIS Kit (Aidlab, Beijing, China).

6. Real-time qRT-PCR detection of an lncRNA

Real-time quantitative reverse transcription-polymerase chain reaction (qRT-PCR) was achieved using 2×SYBR Green Supermix (DBI, Germany) on the qTOWER2.2 real-time PCR System (Analytikjena, Germany) following the manufacturer's instructions. Primers for LUCAT1 and glyceraldehyde 3-phosphate dehydrogenase (GAPDH) were synthesized by Chendu Dangfeng Biotech (Sichuan, China). The primers for LUCAT1 were as follows: forward primer, 5'- CCTCCAGAAACCATGTGTCAA-3' and reverse primer, 5'- GTGAGGAAAGGAGCCAGAAGTC-3'. The primers for GAPDH were as follows: forward primer, 5'- CGGAGTCAACGGATTTGGTC-3' and reverse primer, 5'- CGGTGCCATGGAATTTGCCA-3'. The melting temperature of the LUCAT1 and GAPDH primers was 58°C. The relative expression level for each sample

was calculated as the \log_2 ratio with the Pfaffl method, where $\text{Ratio} = (1 + E_{\text{target}})^{\Delta \text{Ct}_{\text{target (control-sample)}}} / (1 + E_{\text{GAPDH}})^{\Delta \text{Ct}_{\text{GAPDH (control-sample)}}}$ [17, 18]. The sample with the lowest expression level in each group was chosen as the control sample. The reaction efficiencies of the target groups and GAPDH group were both 100%.

7. Cell transfection

ShRNAs specifically targeting the lncRNA LUCAT1 and a scrambled negative control shRNA (shNC) were synthesized by GeneChem Co., Ltd. (Shanghai, China). Following the manufacturer's instructions, Lipofectamine 2000 (Invitrogen, Carlsbad, CA, USA) was used to transfect the shRNAs and their controls into the AGS and SGC-7901 cell lines. The cell state and infection efficiency were observed after transfection.

8. Knocking out LUCAT1 inhibits the proliferation and clone formation of gastric cancer cells

Control shRNA- or LUCAT1-specific shRNA-transfected AGS and SGC-7901 cells (2000/well) were allowed to grow in 96-well plates for 24 hrs after shRNA transfection. After 24h, a CCK8 (Sigma, USA) assay was used to detect cell activity, reflecting cell proliferation. For colony formation, control shRNA- or LUCAT1-specific shRNA-transfected AGS and SGC-7901 cells were plated in a fresh 6-well plate at a density of 1000 cells/well. The inoculated cells were further cultured in an incubator for 14 days, during which time the culture medium was changed every 3 days and the cell status was observed. The cells were fixed with 4% paraformaldehyde and stained with 0.1% crystal violet (Sangon Biotech, Inc., Shanghai, China). The assay was repeated 3 times, and then the clone formation rate was calculated.

9. Flow cytometric analysis of apoptosis and the cell cycle

Control shRNA- or LUCAT1-specific shRNA-transfected AGS and SGC-7901 cells were collected and fixed with 75% ethanol for at least 1 hour. The cells were centrifuged at 321g for 5 min and washed with ice-cold PBS 2 times. Then, the cell cycle dye PI (propidium iodide; Sigma, USA) and RNase were added to the cells for 15 min in the dark at 37°C. The cell cycle was then examined by flow cytometry (Millipore, DE).

After centrifugation at 321 g for 5 min, transfected cells were collected and then resuspended in binding buffer. Apoptosis was detected using Annexin V-APC apoptosis detection kits (eBioscience, CA, USA). Cell apoptosis was detected by flow cytometry (Millipore, DE), and the data were analyzed by guava InCyte software.

10. Transwell Assay

To measure the invasive ability of cells, 500 μL serum-free medium was added to the upper and lower chambers of a Transwell system (Corning, USA), which was placed in an incubator at 37°C for 2 h. After the basement membrane was hydrated, the medium in the upper chamber was removed, and 500 μL cell suspension was added. In the lower chamber, 750 μL 30% FBS medium was added, and the system was cultured in an incubator at 37°C. Then, a cotton swab was used to remove the noninvasive cells in the

chamber, 2-3 drops of a Giemsa (DingguoBiotechnologyCo.,Ltd., Shanghai, China) staining solution was added to the lower surface of the membrane to stain and transfer cells for 3-5 min, and then the chamber was soaked and rinsed several times and air dried. Microscopy (Olympus, Japan) was used to image the attached cells.

11. Wound healing assay

A scratch test was used to assess cell migration. Cells were inoculated into 96-well plates and cultured in an incubator at 37°C and 5% CO₂ for 1 night. The next day, the serum medium was changed to low serum medium, the cells cultured in the 96-well plate were aligned with the center of the lower end of a scratch-making device, and the cells were pushed up slightly to form scratches. Then, the cells were rinsed with serum-free medium 3 times. Photographic images along the scrape line were acquired under a microscope at 0, 6 and 24h.

12. Statistical analysis

Statistical analyses and scientific graphing were performed with the Statistical Product and Service Solutions 22.0 software package (SPSS, Chicago, USA) and GraphPad Prism 7.0 (GraphPad Software, La Jolla, CA), and $P < 0.05$ was considered statistically significant. Associations between the expression levels of lncRNAs and clinicopathologic features were evaluated by a t-test or one-way analysis of variance (ANOVA). Receiver operating characteristic (ROC) curves were established to evaluate diagnostic value.

Results

1. Identification of differentially expressed genes

In the GSE84787 dataset, 83 differentially expressed lncRNAs (absolute fold change > 2 , $p < 0.05$) including 7 downregulated lncRNAs and 76 upregulated lncRNAs were identified by using the limma package in R software (Table S1). Similarly, differentially expressed genes including 70 miRNAs (66 downregulated and 4 upregulated) and 4359 mRNAs (1362 downregulated and 2997 upregulated) were identified in GSE93415 and GSE79973, respectively. A volcano plot was used to visualize aberrant expression between the tumor group and the nontumor group (Figure S2).

2. Construction of an lncRNA-miRNA-mRNA regulatory network

As shown in Figure S3, the interactions between differentially expressed genes (those between miRNAs and lncRNAs and between miRNAs and mRNAs) were predicted by using DIANA-LncBase v2 and mirtarbase. After all repeated interactions were removed, a total of 24 miRNA-lncRNA interactions and 84 miRNA-mRNA interactions were identified (Table SII). Finally, 74 mRNAs, 21 miRNAs and 6 lncRNAs were included in the lncRNA-miRNA-mRNA regulatory network (Figure S1). LUCAT1 (degree=7), hsa-miR-24-3p (degree=14) and IGF1R or KRAS (degree=3) were the lncRNA, miRNA and mRNAs with the largest degrees in the network, respectively, indicating that they were significant genes in the regulatory network. The lncRNA LUCAT1 is probably linked to PAK1 via hsa-miR-377-3p, which is a potential ceRNA regulatory

relationship. According to previous studies, PAK1 is involved in the development and progression of GC [19, 20]. Therefore, we selected the lncRNA LUCAT1 to validate its relationship with GC.

3. LUCAT1 expression was upregulated in GC tissue

The expression levels of LUCAT1 in 70 GC and paired adjacent normal tissue specimens were detected by qRT-PCR. The results revealed that LUCAT1 expression was obviously upregulated in the GC tumor tissue samples compared with the paracancerous tissue samples ($P < 0.001$; Figure. 1B).

4. Clinical characteristics associated with LUCAT1 in GC

The expression level of LUCAT1 and clinicopathological features of GC patients are shown in Table 1, which indicates that the expression pattern of LUCAT1 was associated with tumor diameter ($P < 0.001$), tissue differentiation grade ($P = 0.026$) and LNM status ($P = 0.020$). These results clearly showed that high levels of LUCAT1 expression were associated with aggressive and advanced cancer. However, there were no correlations between the LUCAT1 expression level and other clinicopathological features, including sex and distal metastasis status; however, there was a slight association with the TNM stage ($P = 0.073$).

5. Potential diagnostic value of LUCAT1 in GC

To assess the potential diagnostic value of this lncRNA, a ROC curve was generated to determine the optimal cutoff value. As shown in Figure. 5, the cutoff value for LUCAT1 was 5.4. The area under the ROC curve (AUC) for LUCAT1 was 0.836 ($P < 0.001$, Figure. 1). The sensitivity and specificity were 85.7% and 71.4%, respectively. The Youden index was 0.571.

6. The effect of LUCAT1 on cell proliferation in GC

To investigate the mechanism underlying the involvement of LUCAT1 in malignant GC lesions, we used chemosynthetic shRNAs to knock down endogenous LUCAT1 expression in AGS and SGC-7901 cells and examined the effect of LUCAT1 gene knockout on the proliferation of these human GC cells. The results showed that LUCAT1-shRNA significantly reduced the survival rates of both cell lines compared with a control shRNA (Figure. 2A and B). Moreover, LUCAT1 gene knockout also significantly decreased the colony-formation abilities of the two cell lines (Figure. 2C and D). These results suggest that LUCAT1 may be key in the proliferation of GC cells.

7. ShRNA-mediated knockdown of LUCAT1 expression causes S-phase cell cycle arrest.

To further investigate the effect of LUCAT1 gene knockout on the cell cycle, we used flow cytometry to detect the cell cycle distribution of shRNA-LUCAT1 or control shRNA-transfected AGS and SGC-7901 cells. In the AGS cells transfected with the LUCAT1-specific shRNA, the proportion of S-phase cells was increased (Figure. 3A and 3B). An increase in the proportion of S-phase cells was also observed in the SGC-7901 cells transfected with the LUCAT1-specific shRNA (Figure. 3C and 3D).

8. ShRNA-mediated knockdown of LUCAT1 expression causes apoptosis in GC cells

To confirm that LUCAT1 induces GC cell apoptosis, AGS and SGC-7901 cells transfected with the LUCAT1-specific shRNA were cultured and stained with Annexin V-APC. After a 48-h incubation, apoptosis was detected with the flow cytometric analysis software guava InCyte. We found that the levels of apoptosis in the two groups of LUCAT1-specific shRNA-transfected AGS and sgc-7901 cells were higher than those in the control group (Figure. 3E,3F,3G and 3H). The results showed that LUCAT1 inhibited GC cell apoptosis.

9. Migratory Ability

To investigate whether LUCAT1 affects the migration of GC cells, we conducted a Celigo scratch experiment to detect the migration of AGS and SGC-7901 cells transfected with an shRNA-LUCAT1 virus. After the use of a special scratch-making tool to create scratches, the Celigo assay was used to recognize cells with green fluorescence and acquire images. Then, the images of cells in the same field after migration for different lengths of time were analyzed and processed with software. The results showed that the mobility of the experimental group was significantly lower than that of the control group (Figure. 4).

10. Invasive Ability

We used the AGS and SGC-7901 cell lines to carry out an invasion experiment. We found that the invasiveness of LUCAT1-knockout GC cells was considerably lower than that of control cells group (Figure. 5).

Discussion

lncRNAs are a kind of RNA that lacks coding potential and has a transcript length of more than 200 nucleotides. Comprehensive analysis of lncRNA expression in multiple human organs has shown that the expression patterns of lncRNAs appear to be more tissue-specific than those of protein-coding genes [21], which indicates that specific lncRNAs may be ideal biomarkers for various diseases, especially cancer. In previous studies, many lncRNAs have been significantly correlated with various kinds of cancer.

Sufficient evidence has shown that several lncRNAs are involved in the progression of GC, which is the 4th most common type of cancer and 3rd leading cause of cancer-related death [10, 22]. One typical example is that the lncRNA HOTAIR participates in GC tumorigenesis by acting as a ceRNA that competes for miR-331-3p, whose target is human epithelial growth factor receptor 2 (HER2) [23].

In the ceRNA network established in this study, the lncRNA LUCAT1 is related to PAK1 via the miRNA hsa-miR-377-3p (Figure. S1). According to previous studies, PAK1 is involved in the development and progression of GC [19, 20], suggesting that LUCAT1 may participate in GC tumorigenesis.

Lung cancer-associated transcript 1 (LUCAT1) was first found in the airway epithelium of cigarette smokers and is considered a poor prognostic factor in human non-small cell lung cancer, as it regulates

cell proliferation by epigenetically repressing p21 and p57 expression[24]. Emerging studies indicate that LUCAT1 also promotes tumorigenesis in esophageal squamous cell carcinoma, glioma, clear cell renal cell carcinoma, colorectal carcinoma and breast carcinoma [25-29].

In this study, the real-time qRT-PCR results showed that the expression of LUCAT1 was significantly higher in GC tissue than in paracancerous tissue (Figure. 1B). The ROC curve showed moderate value with high sensitivity (85.7%) and specificity(71.4%) in diagnosing GC. Many early-stage gastric cancer patients choose endoscopic therapy, but even in early-stage gastric cancer patients, a certain proportion of patients have LNM. Therefore, the diagnosis of LNM in gastric cancer intimately affects clinical decision-making. Our study found that LUCAT1 positively correlated with LNM, which may be helpful for the early diagnosis of LNM in gastric cancer. However, LUCAT1 also slightly correlated with TNM stages, perhaps due to our small sample size (Table 1); therefore, the lncRNA Lucat1 may be an ideal biomarker for the early diagnosis and prognosis of GC. In addition, LUCAT1 contributes to malignant biological behaviors in many kinds of cancers[24, 27, 30]. In this study, we also found that knocking down LUCAT1 expression obviously inhibited the proliferation, invasion and metastasis of GC cells and promoted S-phase arrest and apoptosis in GC cells consequently, the detailed mechanisms involving the lncRNA LUCAT1 in the tumorigenesis and metastasis of GC still need to be elucidated in further investigations.

There are several limitations to our study, such as the lack of data related to the relationships between the lncRNA LUCAT1 and overall and disease-free survival rates, which require relatively long observation periods.

Overall, we found obvious differential expression of the lncRNA LUCAT1 in GC through bioinformatics and validated this finding in GC tissue samples. The results indicate that the lncRNA LUCAT1 may emerge as a potential biomarker for the early evaluation of GC diagnosis and prognosis and may play an important role in the development of GC.

Declarations

Acknowledgements

The cell lines used in this study were provided by the the Shanghai Genechem Co., Ltd (Shanghai, China).

Funding

This study were funded from medical and health science and technology project of ZheJiang province(No. 2018245219), and public technology research program from department of science and technology of Zhejiang Province(LGF20H160019).

Availability of data and materials

The datasets used and/or analyzed during the present study are available from the corresponding author on reasonable request.

Authors' contributions

ZZ.Cai, C.Xing, and ZX.Xue conceived and designed the study. YY.Teng ,LY.Ni,HJ.Yu,J.Zhang,LL.Zhou,GR.Lu and YS.Zhu performed the experiments. YY.Teng ,LY.Ni and HJ.Yu wrote the paper. ZZ.Cai and C.Xing reviewed and edited the manuscript. All authors read and approved the manuscript and agree to be accountable for all aspects of the research in ensuring that the accuracy or integrity of any part of the work are appropriately investigated and resolved.

Ethics approval and informed consent

This study was conducted with the approval of the Ethics Committee of The Second Affiliated Hospital and Yuying Children's Hospital of Wenzhou Medical University and was carried out following the guidelines of the Declaration of Helsinki. In addition, informed consent forms were signed by all the participants.

Patient consent for publication

Not applicable.

Competing interests

The authors declare that they have no competing interests.

References

1. Ferlay J, Soerjomataram I, Dikshit R, Eser S, Mathers C, Rebelo M et al. Cancer incidence and mortality worldwide: sources, methods and major patterns in GLOBOCAN 2012. *Int J Cancer*. 2015;136(5):E359-86. doi:10.1002/ijc.29210.
2. Masuda T, Hayashi N, Iguchi T, Ito S, Eguchi H, Mimori K. Clinical and biological significance of circulating tumor cells in cancer. *Mol Oncol*. 2016;10(3):408-17. doi:10.1016/j.molonc.2016.01.010.
3. Ishihara R. Infrared endoscopy in the diagnosis and treatment of early gastric cancer. *Endoscopy*. 2010;42(8):672-6. doi:10.1055/s-0029-1244205.
4. Tanizawa Y, Terashima M. Lymph node dissection in the resection of gastric cancer: review of existing evidence. *Gastric Cancer*. 2010;13(3):137-48. doi:10.1007/s10120-010-0560-5.
5. Ponting CP, Oliver PL, Reik W. Evolution and functions of long noncoding RNAs. *Cell*. 2009;136(4):629-41. doi:10.1016/j.cell.2009.02.006.
6. Tang JY, Lee JC, Chang YT, Hou MF, Huang HW, Liaw CC et al. Long noncoding RNAs-related diseases, cancers, and drugs. *ScientificWorldJournal*. 2013;2013:943539. doi:10.1155/2013/943539.
7. Salmena L, Poliseno L, Tay Y, Kats L, Pandolfi PP. A ceRNA hypothesis: the Rosetta Stone of a hidden RNA language? *Cell*. 2011;146(3):353-8. doi:10.1016/j.cell.2011.07.014.

8. Chan JJ, Tay Y. Noncoding RNA:RNA Regulatory Networks in Cancer. *Int J Mol Sci.* 2018;19(5). doi:10.3390/ijms19051310.
9. Shi X, Sun M, Liu H, Yao Y, Song Y. Long non-coding RNAs: a new frontier in the study of human diseases. *Cancer Lett.* 2013;339(2):159-66. doi:10.1016/j.canlet.2013.06.013.
10. Li T, Mo X, Fu L, Xiao B, Guo J. Molecular mechanisms of long noncoding RNAs on gastric cancer. *Oncotarget.* 2016;7(8):8601-12. doi:10.18632/oncotarget.6926.
11. Irizarry RA, Bolstad BM, Collin F, Cope LM, Hobbs B, Speed TP. Summaries of Affymetrix GeneChip probe level data. *Nucleic Acids Res.* 2003;31(4):e15. doi:10.1093/nar/gng015.
12. Diboun I, Wernisch L, Orengo CA, Koltzenburg M. Microarray analysis after RNA amplification can detect pronounced differences in gene expression using limma. *BMC Genomics.* 2006;7:252. doi:10.1186/1471-2164-7-252.
13. Volders PJ, Verheggen K, Menschaert G, Vandepoele K, Martens L, Vandesompele J et al. An update on LNCipedia: a database for annotated human lncRNA sequences. *Nucleic Acids Res.* 2015;43(8):4363-4. doi:10.1093/nar/gkv295.
14. Paraskevopoulou MD, Vlachos IS, Karagkouni D, Georgakilas G, Kanellos I, Vergoulis T et al. DIANA-LncBase v2: indexing microRNA targets on non-coding transcripts. *Nucleic acids research.* 2016;44(D1):D231-8. doi:10.1093/nar/gkv1270.
15. Chou CH, Chang NW, Shrestha S, Hsu SD, Lin YL, Lee WH et al. miRTarBase 2016: updates to the experimentally validated miRNA-target interactions database. *Nucleic acids research.* 2016;44(D1):D239-47. doi:10.1093/nar/gkv1258.
16. Scardoni G, Petterlini M, Laudanna C. Analyzing biological network parameters with CentiScaPe. *Bioinformatics.* 2009;25(21):2857-9. doi:10.1093/bioinformatics/btp517.
17. Chini V, Foka A, Dimitracopoulos G, Spiliopoulou I. Absolute and relative real-time PCR in the quantification of *tst* gene expression among methicillin-resistant *Staphylococcus aureus*: evaluation by two mathematical models. *Lett Appl Microbiol.* 2007;45(5):479-84. doi:10.1111/j.1472-765X.2007.02208.x.
18. Navidshad B, Liang JB, Jahromi MF. Correlation coefficients between different methods of expressing bacterial quantification using real time PCR. *Int J Mol Sci.* 2012;13(2):2119-32. doi:10.3390/ijms13022119.
19. Qian Z, Zhu G, Tang L, Wang M, Zhang L, Fu J et al. Whole genome gene copy number profiling of gastric cancer identifies PAK1 and KRAS gene amplification as therapy targets. *Genes Chromosomes Cancer.* 2014;53(11):883-94. doi:10.1002/gcc.22196.
20. Liu F, Li X, Wang C, Cai X, Du Z, Xu H et al. Downregulation of p21-activated kinase-1 inhibits the growth of gastric cancer cells involving cyclin B1. *Int J Cancer.* 2009;125(11):2511-9. doi:10.1002/ijc.24588.
21. Derrien T, Johnson R, Bussotti G, Tanzer A, Djebali S, Tilgner H et al. The GENCODE v7 catalog of human long noncoding RNAs: analysis of their gene structure, evolution, and expression. *Genome Res.* 2012;22(9):1775-89. doi:10.1101/gr.132159.111.

22. Xia T, Liao Q, Jiang X, Shao Y, Xiao B, Xi Y et al. Long noncoding RNA associated-competing endogenous RNAs in gastric cancer. *Sci Rep.* 2014;4:6088. doi:10.1038/srep06088.
23. Liu XH, Sun M, Nie FQ, Ge YB, Zhang EB, Yin DD et al. Lnc RNA HOTAIR functions as a competing endogenous RNA to regulate HER2 expression by sponging miR-331-3p in gastric cancer. *Mol Cancer.* 2014;13:92. doi:10.1186/1476-4598-13-92.
24. Sun Y, Jin SD, Zhu Q, Han L, Feng J, Lu XY et al. Long non-coding RNA LUCAT1 is associated with poor prognosis in human non-small lung cancer and regulates cell proliferation via epigenetically repressing p21 and p57 expression. *Oncotarget.* 2017;8(17):28297-311. doi:10.18632/oncotarget.16044.
25. Xiao H, Bao L, Xiao W, Ruan H, Song Z, Qu Y et al. Long non-coding RNA Lucat1 is a poor prognostic factor and demonstrates malignant biological behavior in clear cell renal cell carcinoma. *Oncotarget.* 2017;8(69):113622-34. doi:10.18632/oncotarget.21185.
26. Yoon JH, You BH, Park CH, Kim YJ, Nam JW, Lee SK. The long noncoding RNA LUCAT1 promotes tumorigenesis by controlling ubiquitination and stability of DNA methyltransferase 1 in esophageal squamous cell carcinoma. *Cancer Lett.* 2018;417:47-57. doi:10.1016/j.canlet.2017.12.016.
27. Gao YS, Liu XZ, Zhang YG, Liu XJ, Li LZ. Knockdown of Long Noncoding RNA LUCAT1 Inhibits Cell Viability and Invasion by Regulating miR-375 in Glioma. *Oncol Res.* 2018;26(2):307-13. doi:10.3727/096504017x15088061795756.
28. Zhou Q, Hou Z, Zuo S, Zhou X, Feng Y, Sun Y et al. LUCAT1 promotes colorectal cancer tumorigenesis by targeting the ribosomal protein L40-MDM2-p53 pathway through binding with UBA52. *Cancer Sci.* 2019;110(4):1194-207. doi:10.1111/cas.13951.
29. Zheng A, Song X, Zhang L, Zhao L, Mao X, Wei M et al. Long non-coding RNA LUCAT1/miR-5582-3p/TCF7L2 axis regulates breast cancer stemness via Wnt/beta-catenin pathway. *J Exp Clin Cancer Res.* 2019;38(1):305. doi:10.1186/s13046-019-1315-8.
30. Zheng Z, Zhao F, Zhu D, Han J, Chen H, Cai Y et al. Long Non-Coding RNA LUCAT1 Promotes Proliferation and Invasion in Clear Cell Renal Cell Carcinoma Through AKT/GSK-3beta Signaling Pathway. *Cell Physiol Biochem.* 2018;48(3):891-904. doi:10.1159/000491957.

Table

Table 1 The expression level of LUCAT1 and clinicopathological features of GC patients.

Characteristic	No. of patients (%)	LUCAT1	
		Mean \pm SD	P value
Age (year)			0.6
≤ 60	21(30.0)	7.5 \pm 2.3	
> 60	49(70.0)	7.9 \pm 2.5	
Gender			0.816
Female	25(35.7)	7.8 \pm 2.5	
Male	45(64.3)	7.7 \pm 2.4	
Diameter (cm)			<i><0.001</i>
≥ 4	25(35.7)	6.5 \pm 1.8	
< 4	45(64.3)	8.5 \pm 2.5	
Differentiation			0.026
Well & Moderate	19(27.1)	6.83 \pm 2.42	
Poor	51(72.9)	8.09 \pm 2.39	
Lymphatic metastasis			0.02
N0	23(32.9)	6.8 \pm 2.4	
N1 & N2 & N3	47(67.1)	8.2 \pm 2.3	
Distal metastasis			0.233
M0	65(92.9)	7.7 \pm 2.4	
M1	5(7.1)	9.0 \pm 2.3	
Invasion			0.084
Tis & T1 & T2	19(27.1)	6.9 \pm 2.3	
T3 & T4	51(72.9)	8.1 \pm 2.5	
TNM stage			0.073
I & II	23(32.9)	7.0 \pm 2.3	
III & IV	47(67.1)	8.1 \pm 2.5	

Additional File Legends

Figure S1. An lncRNA-miRNA-mRNA regulatory network in GC. The circular nodes represent mRNAs; the round rectangular nodes represent lncRNAs; and the triangular nodes represent miRNAs. The red nodes represent upregulated genes, and the green nodes represent downregulated genes. Node size represents the degrees, with a larger node corresponding to more degrees.

Figure S2. Differentially expressed genes in GC. The volcano plots of miRNA expression data from GSE93415 (A), lncRNA expression data from GSE84787 (B) and mRNA expression data from GSE79973 (C) are shown separately. The horizontal axis represents \log_2 (fold change), and the vertical axis represents $-\log_{10}$ (P-value). The blue dots represent the selected differentially expressed genes.

Figure S3. Flow chart detailing the ceRNA network analysis.

Figures

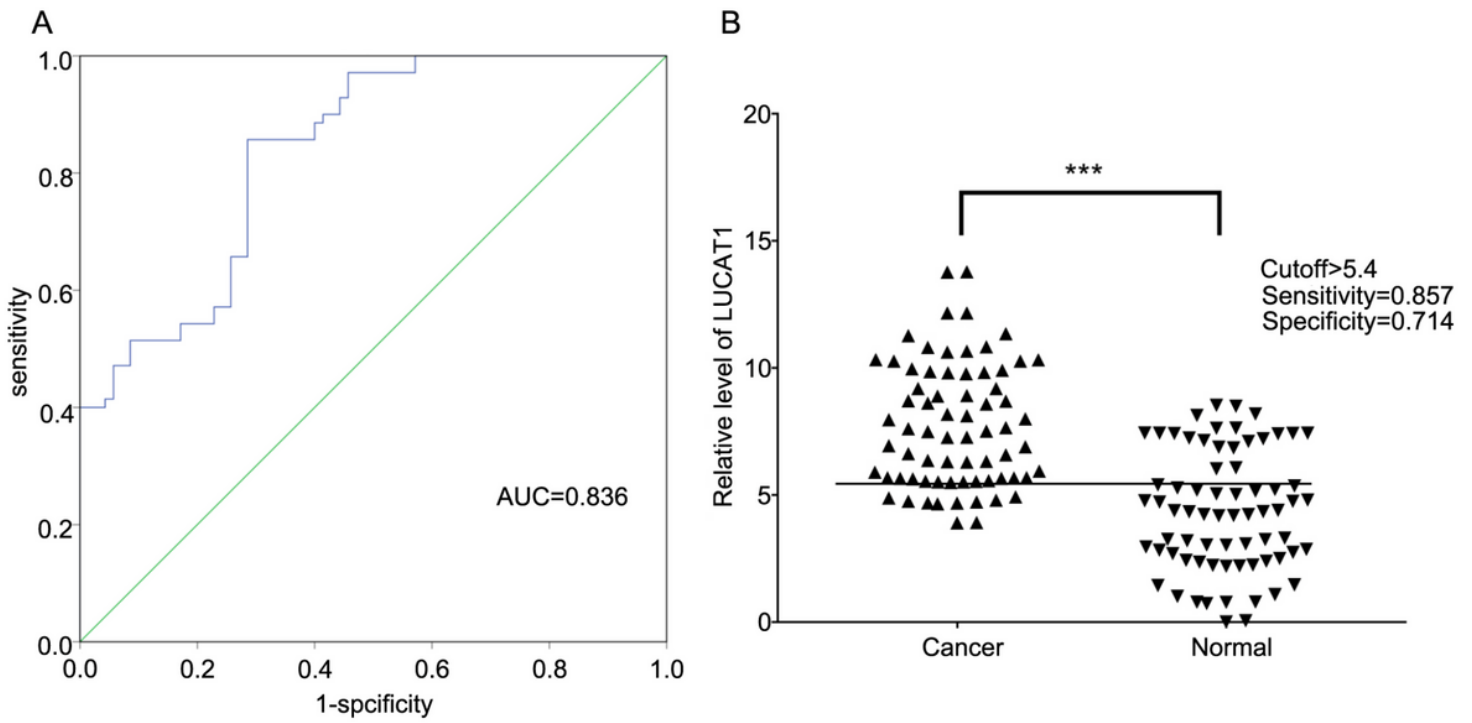


Figure 1

(A)ROC curve for LUCAT1.(B)The expression levels of LUCAT1 in GC samples determined by qRT-PCR. The expression level of LUCAT1 was significantly higher in GC tissue samples than incorresponding nontumor tissue samples($P<0.001$, $n=70$). And the cutoff values for LUCAT1.

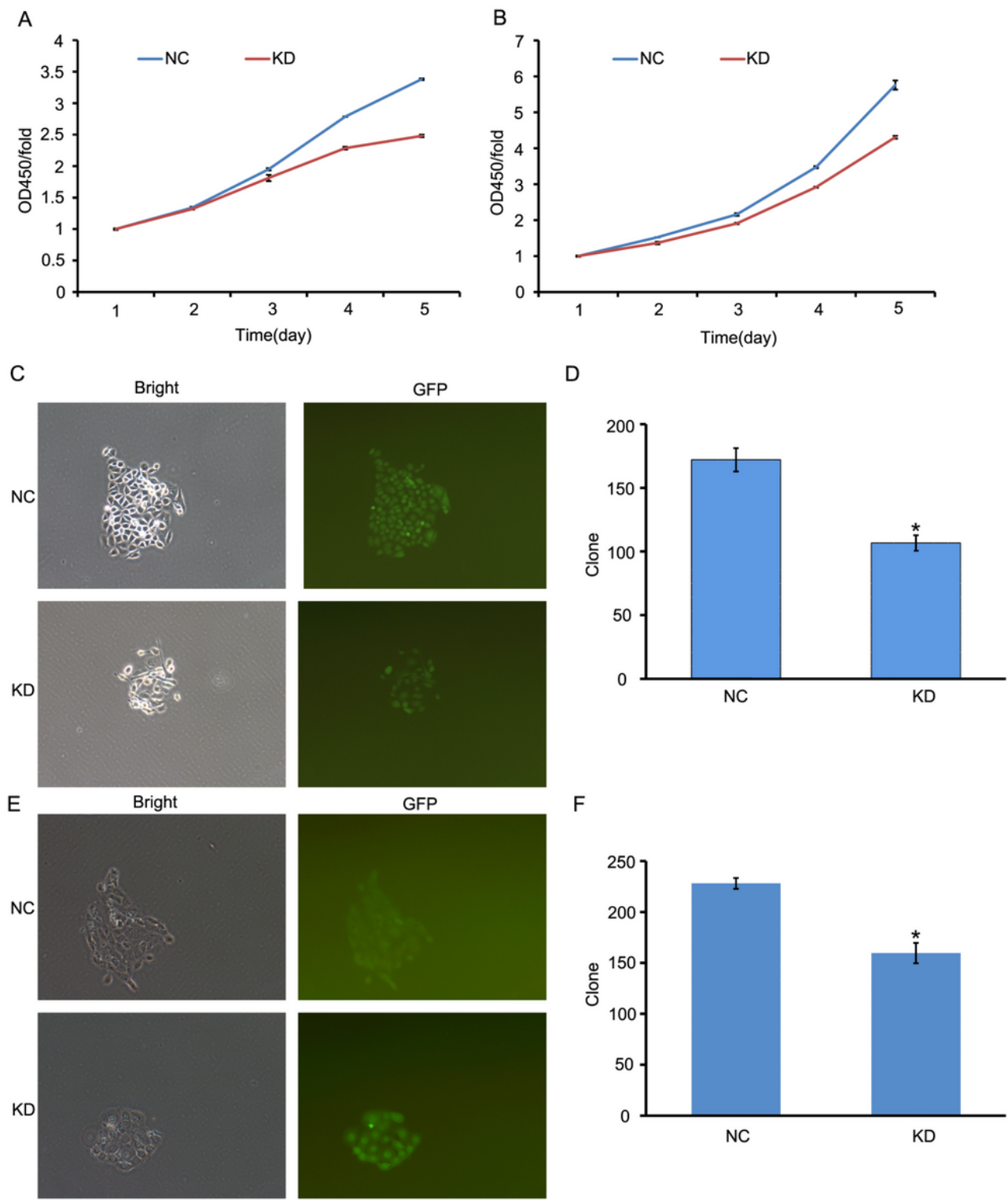


Figure 2

NC represents the control group, and KD represents the representative experimental group. (A) A CCK8 assay was performed to determine the proliferation of AGS cells transfected with a scrambled shRNA (sh-NC) or shRNA-LUCAT1 ($P < 0.05$). (B) A CCK8 assay was performed to determine the proliferation of SGC-7901 cells transfected with the scrambled shRNA (sh-NC) or shRNA-LUCAT1 ($P < 0.05$). (C) Clone-formation experiments were performed to measure the proliferation of AGS cell lines by fluorescence microscopy.

(D) The number of cell clones in the KD group was significantly lower than that in the control group. (E) Clone-formation experiments were performed to measure the proliferation of SGC-7901 cell lines by fluorescence microscopy. (F) The number of cell clones in the KD group was significantly lower than that in the control group. Data are presented as the mean \pm SD of two independent experiments. $P < 0.05$ compared with the NC group.

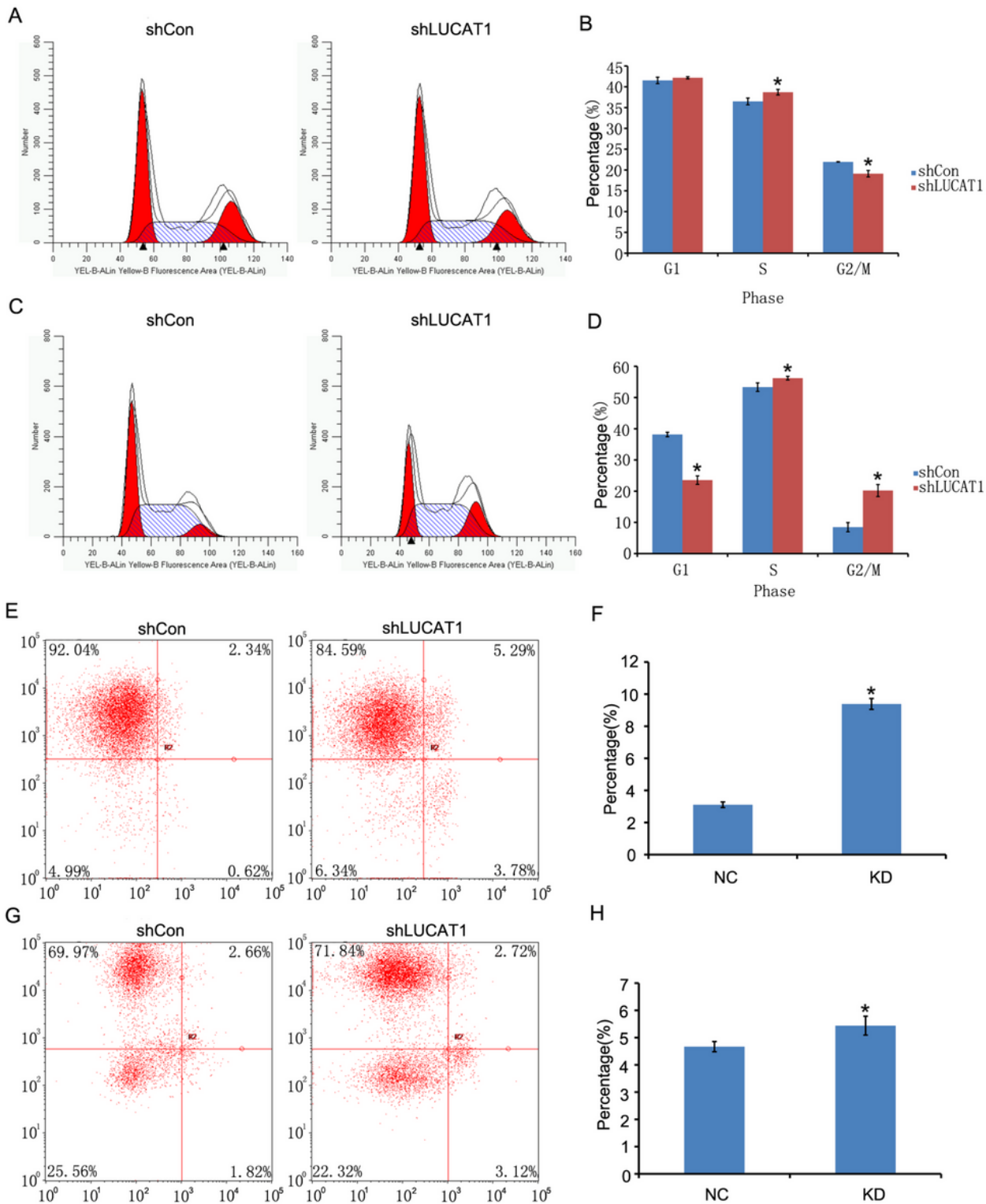


Figure 3

The effects of LUCAT1 on the cell cycles and apoptosis of AGS and SGC-7901 cells in vitro. NC represents the control group, and KD represents the experimental group. (A) and (B) AGS cells were transfected with sh-NC or shRNA-LUCAT1. The DNA content was quantified by flow cytometric analysis. T-tests were performed and indicated that the differences in S- and G2/M-phase cells between the experimental group and control group were significant ($P < 0.05$), but the T-test analysis of G1 cells was nonsignificant ($P > 0.05$). (C) and (D) SGC-7901 cells were transfected with sh-NC or shRNA-LUCAT1. The DNA content was quantified by flow cytometric analysis. T-test analysis indicated that the differences in S-, G1- and G2/M-phase cells between the experimental group and control group were significant ($P < 0.05$). (E) and (F) AGS cells were transfected with sh-NC or shRNA-LUCAT1. The apoptosis rate in the experimental group was significantly higher than that in the control group ($P < 0.05$). (G) and (H) SGC-7901 cells were transfected with sh-NC or shRNA-LUCAT1. The apoptosis rate in the experimental group was significantly higher than that in the control group ($P < 0.05$). Data are presented as the mean \pm SD of two independent experiments. $P < 0.05$ compared with the NC group.

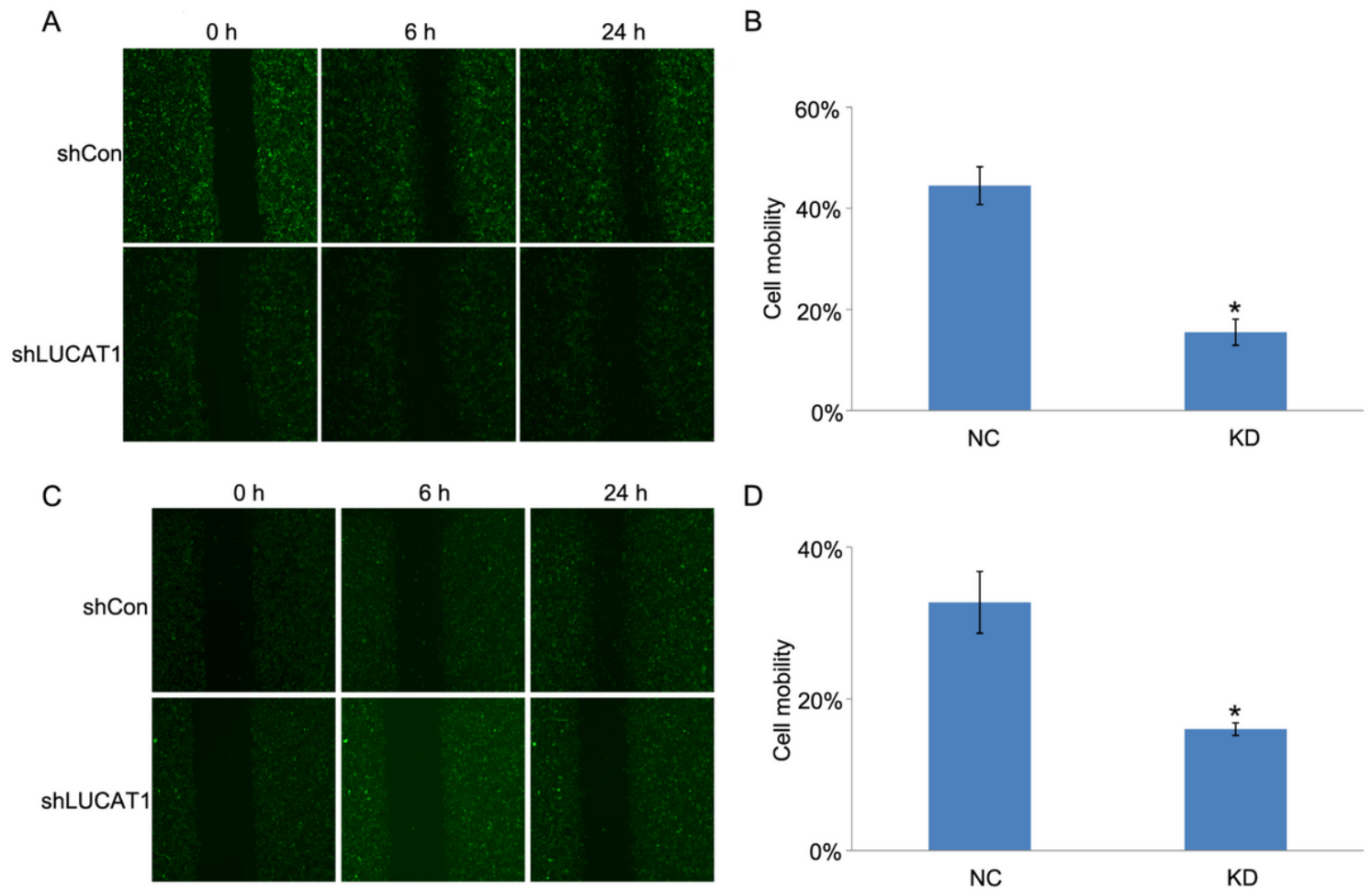


Figure 4

Effects of LUCAT1 on GC cell migration. Cells were observed at 0h, 6h and 24 h. NC represents the control group, and KD represents the experimental group. (A) and (B) AGS cells were transfected with sh-NC or shRNA-LUCAT1. Then, cell mobility was quantified ($P < 0.05$). (C) and (D) SGC-7901 cells were transfected

with sh-NC or shRNA-LUCAT1. Then, cell mobility was quantified ($P < 0.05$). Data are presented as the mean \pm SD of two independent experiments. $P < 0.05$ compared with the NC group.

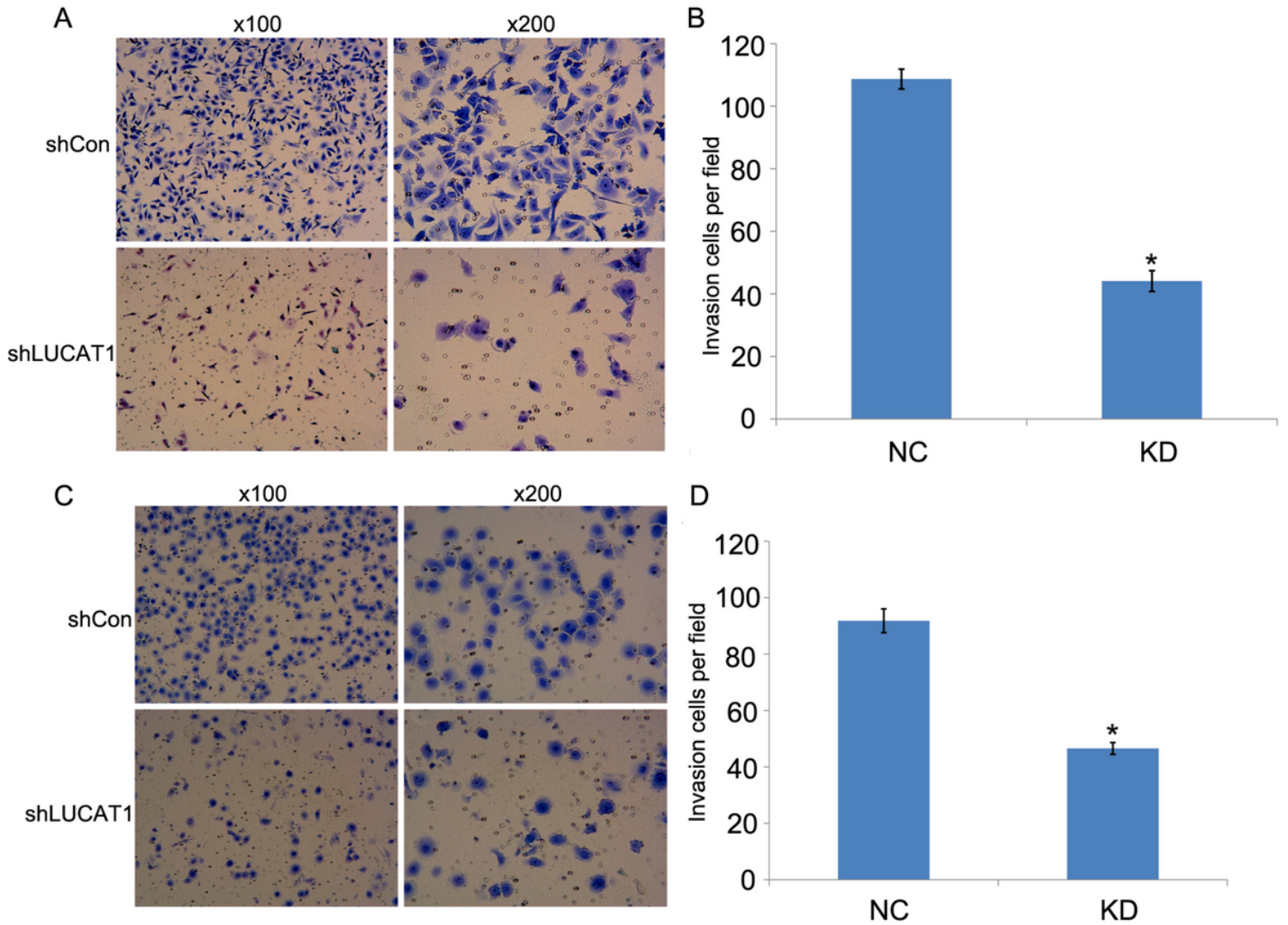


Figure 5

Effects of LUCAT1 on the invasiveness of GC cells. NC represents the control group, and KD represents the experimental group. Images were acquired with an inverted microscope at 100X and 200X. (A) and (B) AGS cells were transfected with sh-NC or shRNA-LUCAT1. The cells were then counted ($P < 0.05$). (C) and (D) SGC-7901 cells were transfected with sh-NC or shRNA-LUCAT1. The cells were then counted ($P < 0.05$). Data are presented as the mean \pm SD of two independent experiments. $P < 0.05$ compared with the NC group.

Supplementary Files

This is a list of supplementary files associated with this preprint. Click to download.

- [TableSI.pdf](#)

- [FigureS2.pdf](#)
- [FigureS1.pdf](#)
- [TableSII.pdf](#)
- [FigureS3.pdf](#)